Maximal Wind Energy Tracing of Brushless Doubly-Fed Generator under Flux Oriented Vector Control

Hicham Serhoud*, Djilani Benattous*

*Institute of Science Technology, University Center of EL-Oued, Algeria

‡Corresponding Author; Hicham Serhoud,BP 476 Gumare, EL-Oued 39400 , Algeria, +213777805237,hserhoud@gmail.com, dbenattous@yahoo.com

Received:18.02.2012Accepted:15.03.2012

Abstract-The aim of this paper is to present the complete modeling and simulation of a grid-connected brushless doubly fed induction generator (BDFG) for variable wind energy conversion is used to assess a maximum power point tracking MPPT strategy for different velocities. The decoupling control of active and reactive powers for BDFG has been developed using PI controllers. The performance of proposed stator power winding flux oriented vector control is examined. The complete system is simulated in the Matlab/Simulink environment and the computer simulation results obtained confirm the effectiveness and validity of MPPT strategy.

Keywords-Brushless doubly fed generator, wind power generation, flux oriented vector control, maximal wind energy capture

1. Introduction

The BDFM which is also known as a self-cascaded machine is composed of two three-phase windings in the stator of different pole numbers (called power winding PW and control winding CW) and a special rotor winding[10].Typically the two stator supplies are of different frequencies, one a fixed frequency supply connected to the grid, and the other a variable frequency supply derived from a power electronic frequency converter (inverter), as illustrated in figure (1), the natural synchronous speed of the machine equal to:

$$\omega_r = \frac{\omega_p \pm \omega_c}{p_p + p_c} \quad (1)$$

Where ω_p and ω_c are the electrical angular velocities of the PW and CW voltages.

Recent research has illustrated the advantages of the brushless doubly-fed machine (BDFM) in motor drive and generator system applications promise significant advantages for wind power generation, as they offer high reliability and low-maintenance requirements by virtue of absence of a brush gear [6].

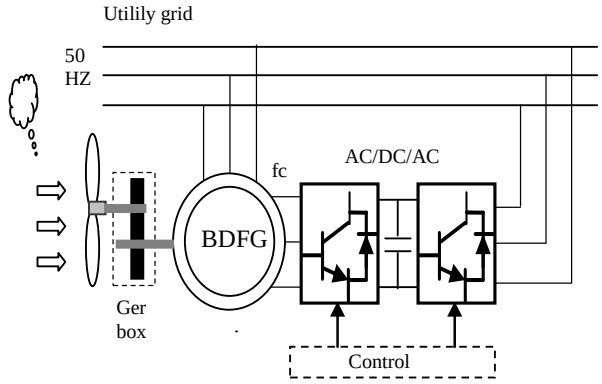

Fig. 1. Configuration of a BDFG wind energy conversion system

This configuration finds an interesting in energy generations applications especially in renewable source, The variable speed constant frequency (VSCF) is the most interesting if the nature of wind with the capability of wind generating systems constantly increasing , it is more important to improve the efficiency by capture the maximum wind energy and use the high quality, efficient and controllable where the major challenge is independent control of active and reactive powers exchanged between the BDFG and the grid.

2. Control Mechanism of the Maximal Wind Energy Capturing

Wind energy is captured by the blades of the wind turbine and is turned into mechanical torque on the hub. from Betz theory, the capture power got from wind energy by wind turbine can be expressed as [16,17]:

$$P = \frac{\pi}{2} C_p R^2 \rho v^3 \quad (2)$$

Where ρ is the air density, R is the turbine radius and the wind velocity, further the power coefficient C_p is a function of the tip speed ratio $(\lambda = \omega_t R / v)$ as well as the blade pitch angle β, ω_t is the angular speed of the wind turbine.

$$C_p(\lambda, \beta) = 0.5176 \left(\frac{116}{\lambda_i} - 0.4\beta - 5\right) e^{-\frac{21}{\lambda_i}} + 0.0068\,\lambda \quad (3)$$

$$\text{Where } \frac{1}{\lambda_i} = \frac{1}{\lambda + 0.08\beta} - \frac{0.035}{\beta^3 + 1} \quad (4)$$

Clearly the turbine speed has to be changed along with wind speed so that optimal tip speed ratio is maintained for maximum power capture and the generator active power matches up to the output power of the turbine.

Figure 2 shows the curve of the power coefficient versus λ for a constant value of the patch angle β . It is clear from this picture that there is a certain value of λ for which C_p is maximized, maximizing thus the power for a given wind speed .

Figure 3 shows the Power- Speed characteristics of the wind turbine, the peak power for each wind speed occurs at the point where C_p is maximized .To maximize the power generated , it is therefore desirable for the generator to have a power characteristic that will follow the maximum $C_{p-\max}$ line.

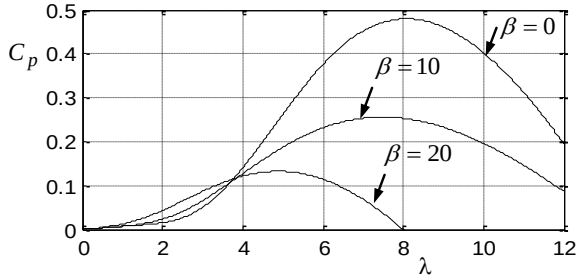

Fig. 2. Wind Turbine Generator $C_p - \lambda$ characteristics

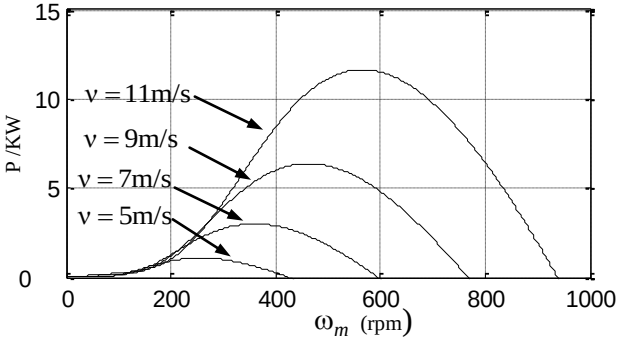

Fig. 3. Wind Turbine Generator power- rotor speed characteristics

To extract the maximum power generated, we must maintain λ at the optimal command rotor speed λ_{opt} .The measurement of wind speed is difficult, an estimate of its value can be obtained:

$$v_{-ref} = \frac{\omega_t R}{\lambda_{opt}} \quad (5)$$

The electromagnetic power must be set to the following value:

$$P_{-ref} = \frac{\pi}{2} C_{p-max} R^2 \rho v_r^3 \quad (6)$$

From the electromagnetic power reference value, it is easy to determine the value of the electromagnetic torque setting:

$$T_{-ref} = P_{-ref} / \omega_t \quad (7)$$

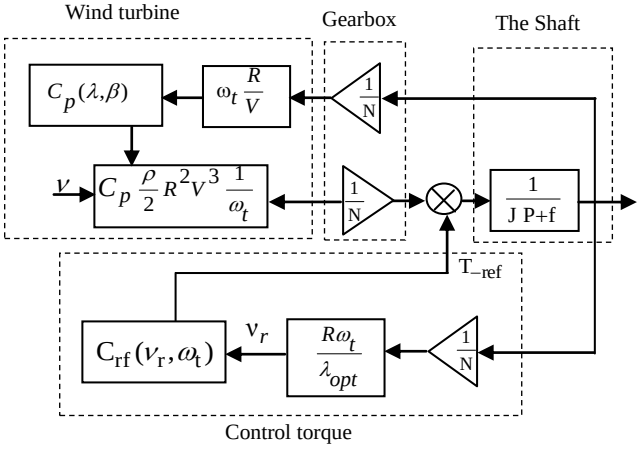

Fig .4. Wind turbine control

3. Mathematical Model

The model in the power winding flux frame is expressed as [4,7,12] :

$$\begin{cases} V_{dp} = R_p.i_{pd} + \dfrac{d\psi_{pd}}{dt} - \omega_p \psi_{pq} \\ V_{qp} = R_p.i_{pq} + \dfrac{d\psi_{pq}}{dt} + \omega_p \psi_{pd} \end{cases} \quad (8)$$

$$\begin{cases} V_{dc} = R_c.i_{dc} + \dfrac{d\psi_{dc}}{dt} - (\omega_p - (P_p + P_c)\omega_r)\psi_{qc} \\ V_{qc} = R_c.i_{qc} + \dfrac{d\psi_{qc}}{dt} + (\omega_p - (P_p + P_c)\omega_r)\psi_{dc} \end{cases} \quad (9)$$

$$\begin{cases} V_{dr} = R_r.i_{dr} + \dfrac{d\psi_{dr}}{dt} - (\omega_p - P_p\omega_r)\psi_{qr} \\ V_{qr} = R_r.i_{qr} + \dfrac{d\psi_{qr}}{dt} + (\omega_p - P_p\omega_r)\psi_{dr} \end{cases} \quad (10)$$

The flux equations are given as:

$$\begin{cases} \psi_{dp} = L_p i_{dp} + M_p i_{dr} \\ \psi_{qp} = L_p i_{qp} + M_p i_{qr} \end{cases} \quad (11)$$

$$\begin{cases} \psi_{dc} = L_c i_{dc} + M_c i_{dr} \\ \psi_{qc} = L_c i_{qc} + M_c i_{qr} \end{cases} \quad (12)$$

$$\begin{cases} \psi_{dr} = L_r i_{dr} + M_c i_{dc} + M_p i_{dp} \\ \psi_{qr} = L_r i_{qr} + M_c i_{qc} + M_p i_{qp} \end{cases} \quad (13)$$

The electromagnetic torque is expressed as [20]:

$$T_e = \frac{3}{2} p_p M_p (i_{qp} i_{dr} - i_{dp} i_{qr}) - \frac{3}{2} p_c M_c (i_{qc} i_{dr} - i_{dc} i_{qr}) \quad (14)$$

The active and reactive powers of power winding are defined as:

$$P_p = \frac{3}{2}(V_{dp} i_{dp} + V_{qp} i_{qp}) \quad (15)$$

$$Q_p = \frac{3}{2}(V_{qp} i_{dp} - V_{dp} i_{dp}) \quad (16)$$

4. Controller Design

4.1. Control of the BDFM With a Power Winding Field Oriented.

If the d-axis of the power winding synchronous reference frame is aligned with the power winding air gap flux the power winding R_p is neglected, then there is relation between the power winding voltage and its flux:

$$\begin{cases} V_{dp} = 0 \\ V_{qp} = V_P = \omega_p \psi_P \end{cases} \quad (17)$$

$$\begin{cases} \psi_P = L_p i_{dp} + M_p i_{dr} \\ 0 = L_p i_{qp} + M_p i_{qr} \end{cases} \quad (18)$$

From (18), the equations linking the rotor currents to the power winding currents are deduced below:

$$\begin{cases} i_{dr} = \dfrac{\psi_P}{M_p} - \dfrac{L_{dp}}{M_p} i_{dp} \\ i_{qr} = -\dfrac{L_{qp}}{M_p} i_{qp} \end{cases} \quad (19)$$

4.2. PW Flux Estimator

Form of PW voltage equation shown (8) its derivation in the stationary reference frame ($\alpha - \beta$ reference frame) is given as follows:

$$\begin{cases} \psi_{\alpha p} = \int (V_{\alpha p} - R_p i_{\alpha p}) dt \\ \psi_{\beta p} = \int (V_{\beta p} - R_p i_{\beta p}) dt \end{cases} \quad (20)$$

The PW flux angle can be expressed as:

$$\theta_p = \arctan \frac{\psi_{\beta p}}{\psi_{\alpha p}} \quad (21)$$

4.3. Control of Power Winding Current:

Suppose that the BDFM is running in steady state, then the dynamic model can be transferred to the state model [7,21] as is following:

$$\begin{cases} V_{dp} = R_p.i_{dp} - \omega_p.L_p i_{qp} - \omega_p M_p i_{qr} \\ V_{qp} = R_p.i_{qp} + \omega_p.L_p i_{dp} + \omega_p M_p i_{dr} \end{cases} \quad (22)$$

$$\begin{cases} \dfrac{s_2}{s_1} V_{dc} = \dfrac{s_2}{s_1} R_c.i_{dc} - \omega_p L_c i_{qc} - \omega_p M_c i_{qr} \\ \dfrac{s_2}{s_1} V_{qc} = \dfrac{s_2}{s_1} R_c.i_{qc} + \omega_p L_c i_{dc} + \omega_p M_c i_{dr} \end{cases} \quad (23)$$

$$\begin{cases} 0 = \dfrac{1}{s_1} R_r.i_{dr} - \omega_p L_r i_{qr} - \omega_p M_c i_{qc} - \omega_p M_p i_{qp} \\ 0 = \dfrac{1}{s_1} R_r.i_{qr} + \omega_p L_r i_{dr} + \omega_p M_c i_{dc} + \omega_p M_p i_{dp} \end{cases} \quad (24)$$

s_1 , s_2 are the slips, which are defined as:

$$s_1 = \frac{\omega_p - p_p\omega_p}{\omega_p}, s_2 = \frac{\omega_c - p_p\omega_p}{\omega_c} \quad (25)$$

Equation (26),(27) can be obtained by combining equation (22) with equation (24) and considering equation (18) ,(20) and neglecting the power winding resistance.

$$i_{dc} = (\frac{L_r L_p - M_p}{M_p M_c}) i_{dp} - \frac{\psi_p L_r}{M_p \omega_p M_c} + \frac{R_r L_p}{M_p M_c \omega_p s_1} i_{qp} \quad (26)$$

$$i_{qc} = (\frac{L_r L_p - M_p}{M_p M_c}) i_{qp} + \frac{R_r \psi_p}{MpM_c \omega_p s_1} - \frac{R_r L_p}{MpM_c \omega_p s_1} i_{dp} \quad (27)$$

Equation (15),(26) represents the relationship of the power current and control wincurrent.

The first term of equation (25) (26) defines the direct coupling between i_c,i_p The second term, performs as a constant and the third term reflects the cross coupling.

4.4. Control of Power Control Current

Combining with equations (09), (12), (19), (24) the control winding voltage can be derived as:

$$V_{dc} = R_c.i_{dc} + (L_c - \frac{M_c^2}{L_r})\frac{di_{dc}}{dt} - \frac{M_c R_r L_p}{\omega_p L_r s_1 M_p}\frac{di_{qp}}{dt} - \frac{M_c M_p}{L_r}\frac{di_{dp}}{dt}$$

$$+ (\omega_p - (p_p + p_c)\omega_r)(L_c i_{qc} + M_c(-\frac{L_{qp}}{M_{p1}} i_{qp}))$$

(28)

$$V_{qc} = R_c.i_{qc} + (L_c - \frac{M_c^2}{L_r})\frac{di_{qc}}{dt} - \frac{M_c R_r L_p}{\omega_p L_r s_1 M_p}\frac{di_{dp}}{dt} - \frac{M_p M_c}{L_r}\frac{di_q}{dt}$$

$$-(\omega_p - (p_p + p_c)\omega_r)(L_c i_{dc} + M_c(\frac{\psi_P}{M_p} - \frac{L_{dp}}{M_p} i_{dp}))$$

(29)

The first term: $R_c.i_{qc} + (L_c - \frac{M_c^2}{L_r})\frac{di_{qc}}{dt}$ shows the relation between V_{qc} with i_{qc}

The second term: $-\frac{M_c R_r L_p}{\omega_p L_r s_1 M_p}\frac{di_{dp}}{dt} - \frac{M_p M_c}{L_r}\frac{di_{qp}}{dt}$ represents the cross coupling it can be neglected in steady state.

The third term:

$-(\omega_p - (p_p + p_c)\omega_r)(L_c i_{dc} + M_c(\frac{\psi_P}{M_p} - \frac{L_p}{M_p} i_{dp}))$ shows another cross coupling, it can be neglected compared with the direct coupling term.

A similar derivation can be applied to the analysis of equation (28) therefore V_c and i_c can be a first order relation.

5. Controller Synthesis

The active and reactive power control strategy for BDFM is described by means of the power winding current, the d-q components of the control winding current are defined in the power winding flux oriented reference frame, with it can be linearly controlled through a proportional-integral (PI) regulator .

We will introduce an additional control loop power level in order to improve the static error, the stator power winding can be controlled by controlling path as shown in Fig (5).

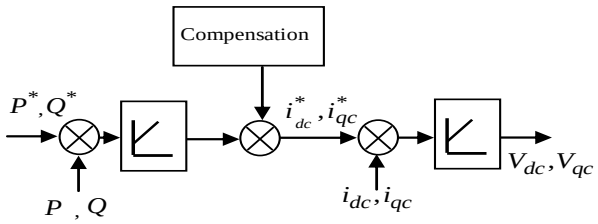

Fig.5. Control scheme

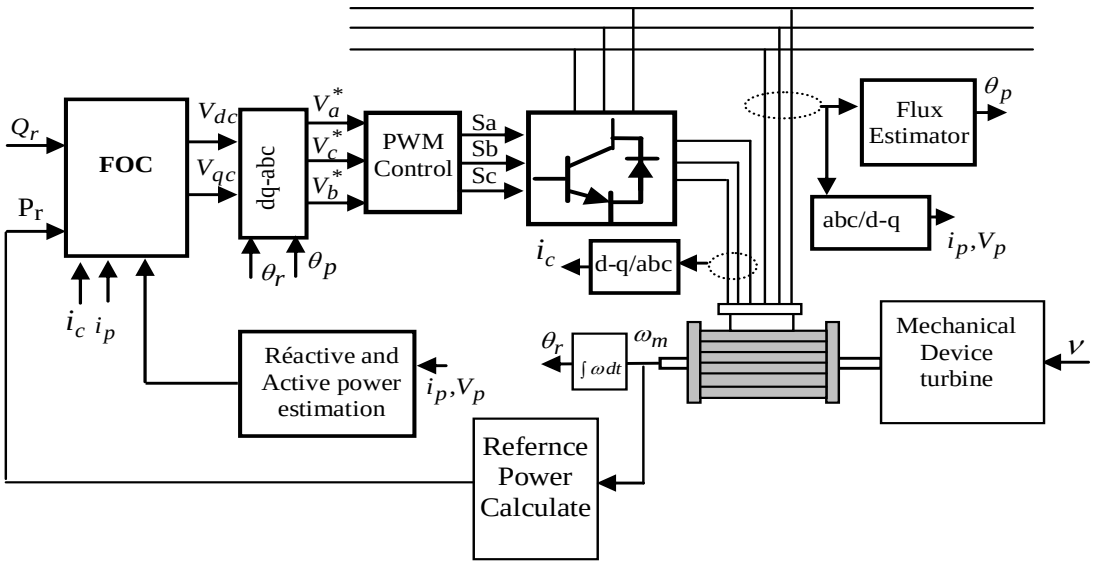

Fig.6. Active and reactive vector control block diagram

6. Simulation Results

The simulation under MATLAB®/Simulink® has been done with a ode 3, fixed-step solver with a step size of 2e-5s. The sample machine used in this simulation model is 3Y-3Y connected and its stator winding is 6-2 pole, the main parameters of BDFM simulation model are reported in Table I, The wind parameters are: $\beta = 0$, $R = 3m$,the optimal tip

speed ratio $\lambda_{opt} = 8.1$,and the corresponding maximum power coefficient $C_{p-\max} = 0.48$,otherwise the speed increase ratio of the gearbox N=2.

To evaluate the dynamic performance of maximum power point tracking of the system proposed a step change in wind speed as shown in Figure 7.

The theoretical optimal angular frequency of BDFM is calculated:

$$\begin{cases} \omega_t = ((60/2\pi)\times\lambda_{opt}\nu)/R \text{ (rpm)} \\ \omega_r = \omega_t N \end{cases} \Rightarrow \quad \omega_r = 51.5662.\nu \quad \text{(rpm)}$$

When wind speed $\nu = 8, 9, 10\ m/s$, the optimal angular electrical frequency are: 412.5, 464, 515.6 (rpm),

In Fig.8 is depicted the optimal command electrical angular speed of rotor and its varies with the variable wind velocity as it is shown in Fig 7.

The active and reactive stator powers and its references are depicted in Fig 9 and Fig 10. These curves represent a good pursuit excepting that the presence of the oscillations during the transient mode.

Fig 7 shows the situation when the wind velocity varies suddenly from 8 m/s to 9 m/s at t= 3s and from v= 9 m/s to 10 m/s at t= 4 s., In both cases, Cp can fast reach around the optimal value. The power coefficient is kept around its optimum Cpmax = 0.48 occurs at a λopt = 8.1as is depicted in Fig.11 and Fig.12.

Fig.13 illustrates the rotor speed- power characteristics of BDFG accorder with the optimal value, these results realize the maximum wind energy tracking control.

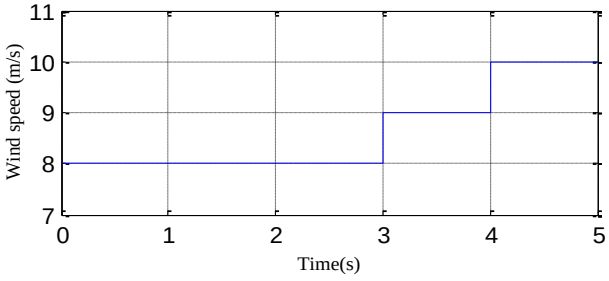

Fig. 7 . Wind speed

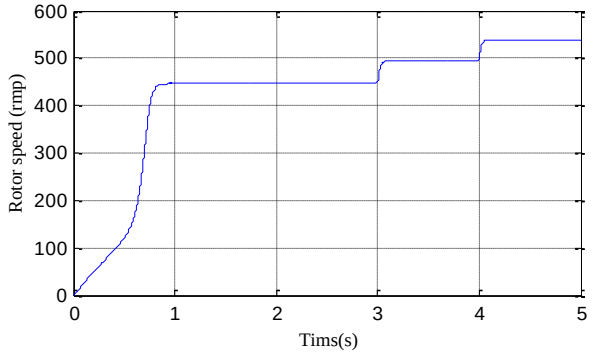

Fig. 8. Rotor speed

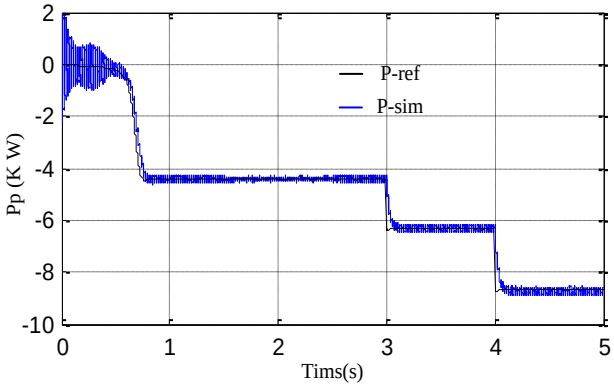

Fig. 9. power winding active power

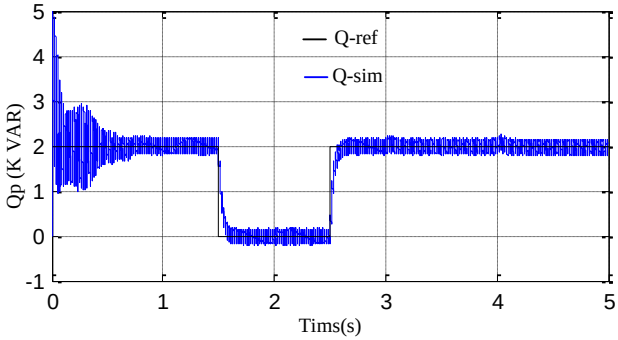

Fig. 10. power winding reactive power

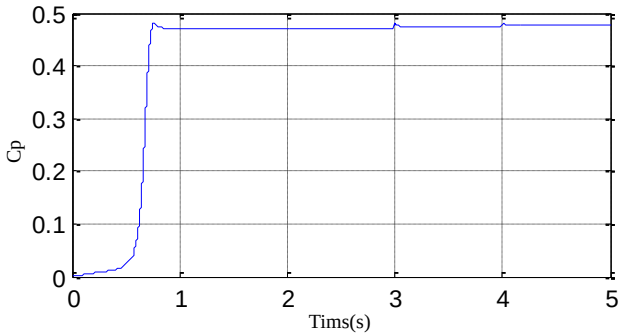

Fig. 11. Power Coefficient Cp variation

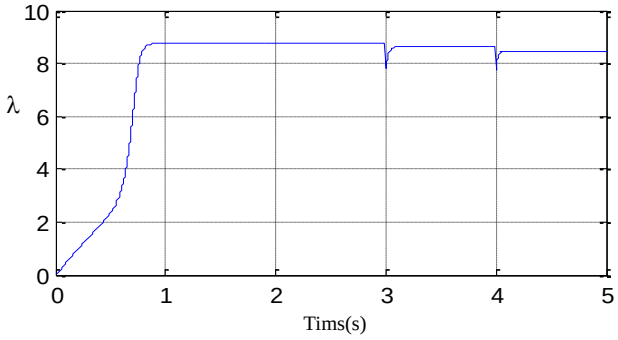

Fig. 12. the tip speed ratio λ

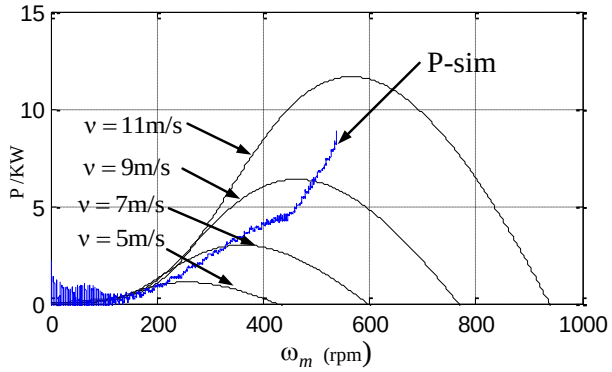

Fig. 13 .Wind turbine maximum power trajectory

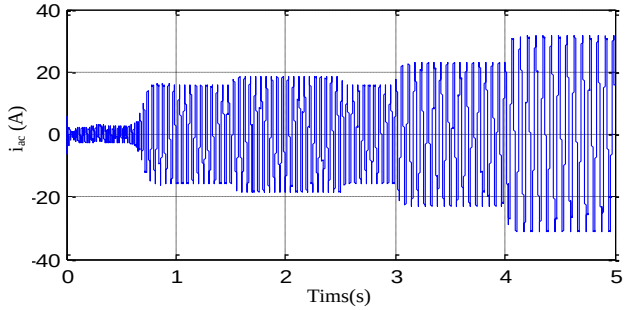

Fig. 14. phase control winding current

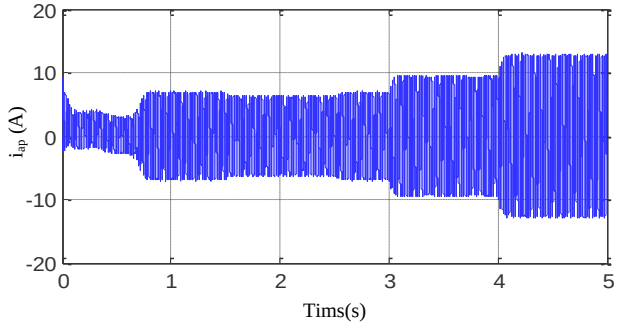

Fig. 15.phase Power winding current

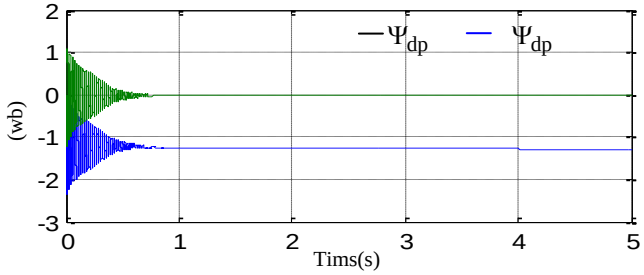

Fig. 16 .Power winding Flux

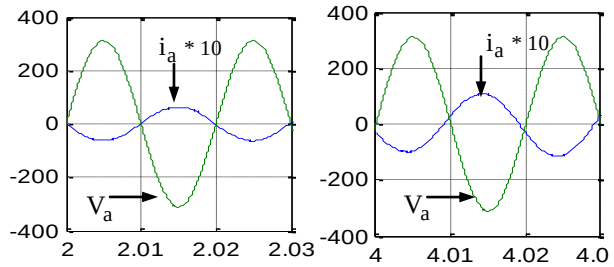

Fig . 17. Zoom of phase power winding current and Voltage

Fig.14 shown the frequency and amplitude of the control winding current both change during the period of the active and reactive power variation, the Fig.15 shown the frequency of power winding current is constants according to power frequency of the grid with amplitude change when the reference of the active and reactive machine power is modified.

In Fig 16, we can see that the power winding flux follows its reference axis (d) with a quadratic component near zero and Fig 17 is the zoom of a stator power winding voltage and the corresponding current shows that the stator power winding current phase changes as a result of increase or decrease of reactive or active winding power demand.

7. Conclusion

In this paper a wind energy conversion system using brushless doubly fed induction generator (BDFG) was presented. The aim of the paper was to develop a strategy of vector control in stator power winding flux oriented of the BDFG based on a control algorithm decoupled of the active and reactive power. The linear PI controllers are used to control both powers and currents and their parameters are initially designed at a specific operating point, the proposed control mechanism of the wind turbine in order to obtain a maximum power is used and The simulation results confirm the validity and effectiveness of the proposed optimal control strategy.

Table 1. The electrical parameters of BDFG

	PW	CW	Rotor
Resistance (Ω)	R_p =0.435	R_c =0.435	R_r = 1.63
self-inductance (mH)	L_p =71.38	L_c =65.33	L_r =142.8
Mutual inductance (mH	M_p =69.311	M_c =60.21	

References

[1] Helio Voltolini, Renato Carlson " Grid Synchronization and Maximum Power Point Tracking for Wind Energy Generation System with Brushless Doubly Fed Induction Generator" IEEE, Industrial Electronics Conference IECOM, pp.2173 – 2177,2008.

[2] Wind-Power Generation System Huang Shoudao, Wang Yi, Wang Yaonan, Ren Guangfa, "Active and Reactive Power Control for Brushless Doubly-Fed Machine 'Power Electronics and Motion Control Conference, 2004. IPEMC 2004. The 4th International

[3] Qi Wang Xiaohu Chen and Yanchao Ji '' Control for Maximal Wind Energy Tracing in Wind Brushless Doubly-Fed Power Generationon System Based Double Synchronous Coordinates''. Proceeding of IEEE Industrial Electronics *Conference, IECON* 2006.

[4] J.Poza , E.Oyarbide ,I.Sarasola M.Rodriguez M.Rodriguez "Vector control design and experimental evaluation for the brushless doubly fed machine" IET Electric Power Applications, July 2008.

[5] Shiyi Shao,Ehsan Abdi and Richard McMaho'' staor – flux –oriented vector for Brushless doubly fed induction

generator'' IEEE Transactions on Industry Electronics ,Vol.56,No.10,October 2009.

[6] Zaskun Sarasola, Javier Poza ,Estanis Oyarbide ,Miguel Angel Rodriguez "Stability Analysis of a Brushless Doubly-Fed Machine under Closed Loop Scalar Current Control" Proceedings of *Industrial* Electronics Conferenc*e* IECON , 2006.

[7] Huang Shoudao Wei Yan Lin Youjie Wang Yaonan ''fuzzy-based power factor control for brushless doubly-fed machines'' Proceedings of the 4th World Congress on Intelligent Control and Automation, June 10-14, 2002, Shanghai. P.R.China.

[8] Yong Liu, Lingzhi Yi, Xiaoyun Zhao "Control of Brushless Doubly-fed Machine for Wind Power Generation Based on Two-stage matrix converter" Proceedings of Power and Energy Engineering Conference, APPEEC 2009.

[9] Longya Xu , Li Zhen and Eel-Hwan Kim '' Field-Orientation Control of a Doubly Excited Brushless Reluctance Machine'' IEEE Transactions on Industry Applications, Vol.34, No.1, January/ February 1998.

[10] J.Poza,E.Oyarbide,D.Roye,andM.Rodriguez, "Unified reference frame dq model of the brushless doubly fed machine," Proc.Inst.Elect. Eng.—Elect-Power Appl., vol. 153,no.5, pp.726–734,Sep. 2006.

[11] J.Poza, E.Oyarbide ,and D.Roye,"New vector control For brushless doubly-fed machines," in Proc .28th Annu, IEEE IECON, Nov. 2002, vol.2, pp .1138 –1143.

[12] M.B.Mohamed, M.Jemli, M-Gossa, K. Jemli." Doubly fed induction generator (DFIG) in wind turbine modelling and power flow control '' International Conference on Industrial Technology (ICIT) IEEE, 2004.

[13] Dendouga, R. Abdessemed, M. L. Bendaas and A. Chaiba" Decoupled Active and Reactive Power Control of a Doubly-Fed Induction Generator (DFIG). Proccedings of the 15th mediterrance conference on control & Automation, July, 2007.

[14] Shi Jin, Fengge Zhang and Yongxin Li,"H ∞ Robust Control for VSCF Brushless Doubly-Fed Wind Power Generator System" proceeding of the IEEE international Conference on Automation and logistics , pp. 471 – 475, 2009.

[15] Fengge Zhang, Shi Jin and Xiuping Wang " L_2 Robust Control for Brushless Doubly-Fed Wind Power Generator " proceeding of the IEEE international Conference on Automation and logistics, pp. 1335 – 1339.,2009.

[16] Yong Liu, Lingzhi Yi, Hongbin Pan , Zhiyong Lan " The simulation study for Brushless doubly-fed generator wind power system based on fuzzy control " IEEE Power and Energy Engineer Conference APPEEC ,pp. 1 - 4 ,2010 .

[17] D.Aouzellag, K.Ghedamsi, E.M.Berkouk " Network Power Flow Control of Variable Speed Wind Turbine" IEEE, Power Engineering ,Energy and Electrical Driver Conference, pp. 435 - 439 ,2007.

[18] J.Poza,"Modélisation, conception et command d'une machine Asynchrone sans Balais Doublement Alimentee pour la Generation a Vitesse Variable," Ph.D.dissertation, Institute National Polytechnique de Grenoble, Oct.2003.

[19] P.C.Poberts,'' A Study of Brushless Doubly-fed (induction) Machines'' PH.D.dissertation, univ. .Cambridge. U.K ,sep 2006.